HHS Public Access

Author manuscript

J Mol Cell Cardiol. Author manuscript; available in PMC 2024 May 30.

Published in final edited form as:

J Mol Cell Cardiol. 2022 February ; 163: 156–166. doi:10.1016/j.yjmcc.2021.10.008.

Individual variability in animal-specific hemodynamic compensation following myocardial infarction

Laura R. Caggiano[a], **Jeffrey W. Holmes**[b], **Colleen M. Witzenburg**[c,*]

[a]Department of Biomedical Engineering, University of Virginia, Charlottesville, VA, USA

[b]School of Engineering, University of Alabama, Birmingham, AL, USA

[c]Department of Biomedical Engineering, University of Wisconsin, Madison, WI, USA

Abstract

Ventricular enlargement and heart failure are common in patients who survive a myocardial infarction (MI). There is striking variability in the degree of post-infarction ventricular remodeling, however, and no one factor or set of factors have been identified that predicts heart failure risk well. Sympathetic activation directly and indirectly modulates hypertrophic stimuli by altering both neurohormonal milieu and ventricular loading. In a recent study, we developed a method to identify the balance of reflex compensatory mechanisms employed by individual animals following MI based on measured hemodynamics. Here, we conducted prospective studies of acute myocardial infarction in rats to test the degree of variability in reflex compensation as well as whether responses to pharmacologic agents targeted at those reflex mechanisms could be anticipated in individual animals. We found that individual animals use very different mixtures of reflex compensation in response to experimental coronary ligation. Some of these mechanisms were related – animals that compensated strongly with venoconstriction tended to exhibit a decrease in the contractility of the surviving myocardium and those that increased contractility tended to exhibit venodilation. Furthermore, some compensatory mechanisms – such as venoconstriction – increased the extent of predicted ventricular enlargement. Unfortunately, initial reflex responses to infarction were a poor predictor of subsequent responses to pharmacologic agents, suggesting that customizing pharmacologic therapy to individuals based on an initial response will be challenging.

Keywords

Hemodynamics; Reflex compensation; Baroreflex; Myocardial infarction; Computational model; Individual variability; Patient-specific; Hypertrophy

*Corresponding author at: 1550 Engineering Drive, Madison, WI 53706-1609, USA. witzenburg@wisc.edu (C.M. Witzenburg).

Appendix A. Supplementary data

Supplementary data to this article can be found online at https://doi.org/10.1016/j.yjmcc.2021.10.008.

Disclosure and Conflicts of Interest

The authors have nothing to disclose and declare no conflicts of interest.

1. Introduction

About 85% of the 800,000 Americans who suffer a heart attack (myocardial infarction, MI) annually survive the initial event [1]. Survivors often have reduced cardiac function, however, and increased risk of hypertrophy and heart failure. Importantly, post-infarction heart failure is common (incidence of 16–30%, [2,3]) and difficult to treat (1-year mortality of 31–45%, [2,4]). A number of metrics have been proposed to prospectively estimate heart failure risk including a range of biomarkers (such as cytokines and matrix metalloproteinases [5]) as well as various functional metrics (such as ventricular volume and ejection fraction [6–8]). While risk stratification is crucial for patient planning and treatment, no one factor or set of factors has been determined that predicts heart failure risk well [9–11]. In fact, although post- infarction remodeling correlates broadly with infarct size, both echocardiographic [12] and MRI [13] studies show striking variability in the degree of eccentric hypertrophy for any given infarct size, particularly among patients with moderately sized infarcts (15–25%).

Multiple processes, including both neurohormonal activation and altered biomechanics, interact through a network of intracellular signaling cascades to drive the development of post-infarction hypertrophy. Many of the signals known to activate hypertrophy are associated directly or indirectly with the sympathetic reflexes triggered by infarction [14–16], suggesting that individual variability in sympathetic activation might account for some of the observed variability in remodeling. While sympathetic activation can directly activate intracellular pathways that stimulate myocyte hypertrophy, it also indirectly modulates hypertrophic stimuli by altering ventricular loading. Post- infarction compensatory reflexes sense blood pressure through baroreceptors in the carotid arteries and act to preserve mean arterial pressure through an increase in heart rate, an increase in contractility of the surviving myocardium, arterial vasoconstriction, and venous vasoconstriction. Other stretch-mediated reflexes can modulate the baroreceptor response acutely [17,18], while the kidneys provide long-term regulation of blood volume following infarction [19,20]. In our recent study [21], we developed a method to identify the balance of post-infarction compensatory mechanisms employed by individual animals following infarction based on measured hemodynamics. We found marked variability in post-infarction reflex compensation in a published canine study, and postulated that this could contribute to variability in ventricular remodeling and provide a target for individualizing therapies aimed at reducing that remodeling.

Here, we conducted prospective studies of acute myocardial infarction in rats to test the degree of variability in reflex compensation as well as whether responses to pharmacologic agents targeted at those reflex mechanisms could be anticipated in individual animals. We confirmed that individual animals use very different mixtures of reflex compensation in response to experimental coronary ligation. Furthermore, some of those compensatory mechanisms – such as venoconstriction – tend to elevate left ventricular volumes and increase peak circumferential stretch in the surviving region of the ventricle, which according to both experimental studies [22,23] and predictive models [24–26] is a stimulus for left ventricular enlargement, while other mechanisms – such as increased contractility – act to reduce peak circumferential stretch and expected risk of enlargement. Unfortunately, initial reflex responses to infarction were a poor predictor of subsequent responses to

pharmacologic agents, suggesting that customizing pharmacologic therapy to individuals based on an initial response will be challenging.

2. Methods

We performed acute myocardial infarction experiments in rats, measuring hemodynamics prior to myocardial infarction, following myocardial infarction, and in response to pharmacologic agents. Using a computational model, we fitted hemodynamic measurements in order to examine the degree of variability in the postinfarction hemodynamic compensation mechanisms individual animals employed. Then, we perturbed hemodynamics pharmacologically and quantified the effects on compensation. Finally, we estimated the degree to which differences in the stretch of the surviving region would be expected to produce an increase or decrease in eccentric hypertrophy based on established predictive models of cardiac remodeling.

2.1. Surgical procedures and data collection

We created transmural anteroapical infarcts in adult male Sprague- Dawley rats (369 ± 48 g) by permanent ligation of the left anterior descending coronary artery. All studies were performed in accordance with the Guide for the Care and Use of Laboratory Animals and approved by University of Virginia's Institutional Animal Care and Use Committee. Animals were anesthetized with isoflurane in 100% O2 (3.0% induction, 1.5–2.0% maintenance), intubated via tracheotomy, and ventilated with positive-pressure ventilation. Body temperature was maintained with a warming pad. The chest was opened via midline sternotomy with careful attention to hemostasis. Instrumentation was similar to our previous studies [22,27]. Prior to ligation of the left anterior descending coronary artery, four 1.0 mm sonomicrometer crystals (Sonometrics, London, Ontario, Canada) were sewn to the epicardial surface of the left ventricle with 6–0 silk suture: on the posterior wall two-thirds of the distance from apex to base and just lateral to the intraventricular groove (posterior); 2) on the anterior wall two-thirds of the distance from apex to base and just lateral to the intraventricular groove (anterior); 3) on the lateral wall under the left atrial appendage (base); and 4) at the left ventricular apex (apex). A Millar SP-671 pressure transducer (Millar Instruments, Houston, Texas) was inserted into the left ventricular cavity through a hole created with a 25-gauge needle in the anterior wall. Left ventricular segment lengths and pressure data were acquired at 312 Hz using the commercial software SonoLab (Sonometrics). A total of 22 adult male Sprague-Dawley rats were used for these studies. Rats were excluded from data analysis if no infarct was detected ($n = 3$), if pressure tracings were of poor quality ($n = 3$), or in the case of acute mortality ($n = 3$); data from the remaining 13 animals are reported here.

We measured left ventricular pressure and segment lengths at five time points in each rat (Table 1). Following a control reading (time point 1), we created transmural anteroapical infarcts by permanent ligation of the left anterior descending coronary artery [28]. Thirty minutes following ligation, hemodynamic measurements were again recorded (time point 2). Next, we injected either dobutamine (4 μg/kg) or nitroglycerin (20 μg/kg) into the right ventricle and recorded pressure and segment lengths of the left ventricle (time point 3).

We selected these agents specifically to target the compensatory mechanisms that cannot be measured directly post-infarction in order to test the ability of our computational model to correctly identify their effects. At low doses, the beta-adrenergic agonist dobutamine induces a large increase in myocardial contractility with minimal change in heart rate [29,30]. Similarly, at low doses, nitroglycerin is a potent venoselective vasodilator [31–34]. The high clearance rates of dobutamine and nitroglycerin enabled us to quantify their effects serially in each rat. Following the transient pharmacologic response (~5 min after injection) to each agent, an additional postinfarction baseline recording was made. We randomized animals to dobutamine or nitroglycerin first and waited several minutes between pharmacologic agents. For each experimental condition, we also took hemodynamic measurements over a range of preload pressures by temporarily occluding the inferior vena cava [22]. Supplemental Fig. 2A and B show the end-systolic and end-diastolic pressure-volume behavior observed during inferior vena cava occlusion in a representative rat.

After each study, the heart was arrested by retrograde aortic perfusion with a cold cardioplegic solution (2,3-butanedione monoxime in phosphate-buffered saline [35]) containing fluorescent microspheres [36] and removed. The atria were trimmed away, and overall dimensions as well as the positions of the sonomi- crometers were measured and recorded. The sonomicrometers were then removed, and the left and right ventricles were weighed. Next, we suspended the left ventricle in the cold cardioplegic solution and filled the left ventricular cavity with an agarose gel (0.4 g agarose per 10 ml DI water). The left ventricle was sectioned into 2 mm-thick short-axis slices. Fig. 1 shows short-axis slices of the left ventricle of a representative animal under ultraviolet light. There was clear demarcation between regions with microspheres (bright yellow) and those without (black). Images of both the basal and apical sides of each slice were segmented manually and reconstructed to determine the total left ventricular wall volume as well as the percentage of the wall volume that was infarcted, IS.

2.2. Data analysis

Base-apex (BA) segment length, anterior-posterior (AP) segment length, and ventricular pressure were exported for analysis via a series of custom routines written in MATLAB detailed in our previous studies [22,35]. Briefly, the volume enclosed by the epicardial surface, V, was computed from the segment lengths assuming a truncated ellipsoidal geometry for the left ventricle, $V = 1.125 * \left(\pi/6\right) AP^2 BA$. Wall volume was computed from the mass of the left ventricle assuming a density of 1.06 g/cm^3 for myocardium [37,38]. To obtain the cavity volume of the left ventricle we subtracted wall volume from the epicardial volume. For each cardiac cycle, end diastole was selected as the point immediately preceding the rapid pressure upstroke and end systole as the point when the ratio of left ventricular pressure to cavity volume was maximized. Beginning of ejection was selected as the point between end diastole and end systole immediately preceding rapid volume loss. Data from approximately 30 beats were averaged for each experimental hemodynamic state.

We combined end-systolic points from the control state with and without inferior vena cava occlusion to form a control end-systolic pressure-volume relationship. A line is typically used to estimate the end-systolic behavior of an intact ventricle [39,40]. Thus, we assumed

$$P_{ES} = E(V_{ES} - V_0), \tag{1}$$

and estimated E, the end-systolic elastance, and V_0, the unloaded volume for this relationship. Acutely, the end-diastolic behavior of the ventricle is unchanged by the pharmacologic agents employed here or by myocardial infarction [41]. Therefore, end-diastolic points from all experimental conditions with and without inferior vena cava occlusion were combined to form the overall end-diastolic pressure-volume relationship. We assumed exponential end-diastolic behavior [42,43], where

$$P_{ED} = Bexp[A(V_{ED} - V_0)] - B. \tag{2}$$

Using the previously determined value for V_0, we estimated coefficients A and B for the end-diastolic pressure-volume relationship.

For each experimental condition, heart rate, HR, and arterial pressure were determined from ventricular pressure tracings. Similar to our previous study [21], we estimated arterial pressure by assuming it was the same as left ventricular pressure during ejection and linearly interpolating for the remainder of the cardiac cycle. Then, we computed the mean arterial pressure, MAP. We computed systemic vascular resistance, SVR, as

$$SVR = \frac{MAP}{HR * SV}, \tag{3}$$

where stroke volume, SV was computed as the difference between the left ventricular end-diastolic and end-systolic volumes.

2.3. Computational model

We adapted our previously published compartmental model of postinfarction canine hemodynamics for rats [21,44]. Supplemental Fig. 1 shows a schematic of the model. Briefly, ventricular contraction was simulated using time-varying elastance, systemic and pulmonary vessels were represented by capacitors in parallel with resistors, and pressure-sensitive diodes acted as valves. To simulate myocardial infarction the damaged left ventricle was functionally divided into two compartments: a noninfarcted, contractile compartment, and an infarcted, non-contractile compartment. At any time point during the cardiac cycle, the pressures within these compartments were the same and their volumes added to the total left ventricle volume (see Supplemental Section S.1 for details).

We modeled hemodynamics in dogs in our previous studies [21,25]. Therefore, to simulate hemodynamics in rats, model parameters that were not directly measured, computed from measurements, or fit to measured data were estimated by allometrically scaling published parameters from a dog weighing ~20 kg to a rat weighing ~0.4 kg. Allometric scaling

describes the dependence of a biological variable on body mass with a scaling exponent, b [45]. Many experimental and theoretical analyses have been performed to quantify cardiovascular scaling exponents [45–47]. We scaled model resistances by $b = -3/4$ based on theoretical and empirical measurements of total peripheral resistance. The dependence of capacitance on vessel dimensions dictates it scales linearly [48,49]. Supplemental Table 1 shows all scaled model parameters.

Four model parameters reflect the primary hemodynamic compensations that occur in response to myocardial infarction: heart rate (HR), systemic vascular resistance (SVR), end-systolic elastance of the non- infarcted compartment (E_n), and stressed blood volume (SBV). When determining the animal-specific parameters associated with hemodynamic compensation we first considered the control hemodynamic state. Heart rate was determined from the ventricular pressure tracings and prescribed directly in the model. Systemic vascular resistance changes with arterial vasoconstriction and was estimated according to eq. 3. For an intact ventricle, contractility is typically quantified by the slope of the end-systolic pressure-volume behavior [39,40]. Therefore, prior to infarction, we estimated the end-systolic elastance from the measured end-systolic pressure-volume points according to eq. 1. Venous vasoconstriction changes the size of the stressed blood pool within the circulation. Direct measurement of changes in stressed blood volume are challenging during *in vivo* experiments because they require circulatory arrest [50,51]. Therefore, for the control time point, we initialized SBV at its scaled value, 5 ml, and utilized the model to fit SBV by minimizing the sum squared error in left ventricular end-diastolic volume using the fminsearch function in MATLAB. We showed previously that the pressure-volume behavior of left ventricular at end diastole is highly sensitive to SBV [21]. Systemic characteristic resistance was initialized at 2% of SVR and fit using the model by minimizing the sum squared error in mean ventricular pressure during ejection. Supplemental Fig. 2 shows a representative example of the model fitting process.

For the control time point, end-systolic elastance quantifies the myocardial inotropic state of the entire left ventricle since no infarct is present. In an infarcted heart, however, this slope depends not only on the behavior of the surviving contractile myocardium but also on the size and behavior of the non-contractile infarct region. Thus, for all the remaining experimental time points E_n could not be directly fit to the data. For these time points, we utilized the model to fit both SBV and E_n by minimizing the sum squared error in the left ventricular end-diastolic and end-systolic volumes. SBV and E_n were initialized at their control values. Again, heart rate was determined from the ventricular pressure tracings and prescribed directly in the model and systemic vascular resistance was estimated according to eq. 3. For both the control time point and all myocardial infarction time points, we were able to compute the time course of elastance throughout the cardiac cycle for each rat directly (see Supplemental Section S.2 for details). To compare the contractility of the surviving myocardium with the non-infarcted control from the model, the control value was simply multiplied by $(1 - IS)$. Again, systemic characteristic resistance was initialized at 2% of SVR and fit using the model by minimizing the sum squared error in mean ventricular pressure during ejection.

2.4. Hypertrophic mechanical stimuli

In our previous publication [24], we evaluated the ability of various mechanical stimuli to simulate eccentric and concentric ventricular hypertrophy following volume and pressure overload, respectively, and found differences in stretch to be the most successful. Subsequently, we successfully utilized the differences in peak stretches in the circumferential and radial directions within a computational model of ventricular growth to predict average ventricular dimensions in dogs following myocardial infarction [21,25]. Peak circumferential stretch occurred at end-diastole and was predictive of ventricular enlargement. Peak radial stretch occurred at end-systole and was predictive of ventricular thickening and thinning. To account for changes in geometry with growth we developed analytic expressions based on the relationships between strain and volume and stress and pressure in a thin-walled sphere. Circumferential and radial stretches were defined as the ratio of the loaded circumference to the unloaded circumference and the loaded thickness to the unloaded thickness, respectively. The unloaded dimensions are modified when simulating growth. Therefore, we computed circumferential stretch in the noninfarct region as

$$\lambda_c = \sqrt[3]{\frac{V_n}{(1-IS)V_0}}, \tag{4}$$

where V_n was the volume in the noninfarct region of the left ventricle from the model. Within the model, the unloaded thickness of the noninfarct region of the left ventricle was

$$h_{n0} = \sqrt[3]{\frac{3}{4\pi}(1-IS)*(V_0+V_{wall})} - \sqrt[3]{\frac{3}{4\pi}(1+IS)V_0}, \tag{5}$$

where V_{wall} was the wall volume of the total left ventricle, and the loaded thickness of the noninfarct region of the left ventricle was

$$h_n = \sqrt[3]{\frac{3}{4\pi}((1-IS)V_{wall}+V_n)} - \sqrt[3]{\frac{3}{4\pi}V_n}. \tag{6}$$

Thus, radial stretch in the noninfarct region was computed as

$$\lambda_r = \frac{h_n}{h_{r0}} \tag{7}$$

To explore how variability in hemodynamic compensation could affect subsequent ventricular hypertrophy in our rats we compared the maximum circumferential and radial stretches both between rats and with pharmacologic perturbation.

2.5. Statistics

Statistical analysis was performed using GraphPad Prism 8. We conducted D'Agostino-Pearson omnibus K2 tests to test for normality of hemodynamic data for each time point. For metrics that passed the normality test, paired parametric *t*-tests were used to determine if changes were significantly different between time points. Otherwise, Wilcoxon matched-pairs signed rank tests were used. When evaluating if relationships between metrics were significant we computed two-tailed Pearson correlation coefficients or nonparametric Spearman correlation coefficients from linear regression. We also tested for homoscedasticity.

3. Results

Data from 13 acutely infarcted rats was analyzed to assess the variability in compensatory responses postinfarction. Fig. 2 shows measured and simulated pressure-volume behavior for a representative animal for all experimental time points. In the majority of rats, infarction shifted the pressure-volume behavior rightward whereas pharmacologic perturbation shifted it leftward. The model matched the experimental data well for all conditions.

Passive ventricular parameters were estimated directly from the data for each rats. Supplemental Fig. 2A and B details this process for a representative rat. At the control time point, HR and SVR were computed directly from experimental measurements. E was estimated from inferior vena cava occlusion end-systolic pressure-volume behavior and was equivalent to E_n. We fitted SBV, the parameter associated with venoconstriction, based on the sum squared error in left ventricular end-diastolic volume (see Supplemental Fig. 2C for example). Then, systemic characteristic resistance was fitted using the model by minimizing the sum squared error in mean ventricular pressure during ejection (see Supplemental Fig. 2D for example). The final model fits produced control end- diastolic volumes, end-systolic volumes, and mean pressures during ejection, within 0.0005 ml, 0.005 ml, and 1.3 mmHg of the measured values for all rats, respectively. For all other time points, HR and SVR were again computed directly from experimental measurements. We fitted SBV and E_n, the model parameter associated with contractility of the noninfarcted region, by minimizing the sum squared error in the end-diastolic and end-systolic left ventricular volumes (see Supplemental Fig. 2E for example). Next, systemic characteristic resistance was fitted using the model by minimizing the sum squared error in mean ventricular pressure during ejection (see Supplemental Fig. 2F for example). The final model fits produced postinfarction end-diastolic volumes, end-systolic volumes, and mean pressures during ejection, within 0.006 ml, 0.005 ml, and 3.0 mmHg of the measured values for all rats, respectively.

3.1. Postinfarction hemodynamic compensation

Consistent with our previous findings [21], the mix of compensatory responses employed by individual animals was highly variable postinfarction (Fig. 3). For example, the rat represented in hot pink compensated almost exclusively with venoconstriction (increasing SBV and decreasing SVR and E_n), while the rat represented in navy maximized myocardial contractility (increasing E_n with moderate changes in SVR and SBV). Most rats exhibited an increase in systemic vascular resistance and, on average, SVR increased (paired parametric

t-test, $p < 0.001$). Changes in heart rate were small, ranging from − 6 to 11%. Most, but not all, rats were able to maintain MAP within 15% of baseline even in the presence of an acute infarct.

We computed the correlation coefficients for each pair of compensatory mechanisms to quantify their interactions. There was a significant negative relationship between the change in SBV and the change in E_n postinfarction (Fig. 4). Thus, animals that compensated strongly with venoconstriction tended to exhibit a decrease in the contractility of the surviving myocardium and those that compensated strongly with myocardial contractility tended to exhibit venodilation. No other mechanism pairs were significantly correlated and all pairs passed the test for homoscedasticity ($p > 0.05$). Next, we computed the squared correlation coefficient between infarct size and each compensatory mechanism to quantify the relationship between injury severity and compensation. Infarct size ranged from 8 to 38% of the total left ventricle wall volume. No correlation coefficient was statistically significant, indicating that there was no trend in the change in heart rate, systemic vascular resistance, end-systolic elastance of the surviving myocardium, or stressed blood volume with infarct size (Supplemental Fig. 3).

3.2. Pharmacologic agents

As anticipated, following the postinfarction administration of nitroglycerin there was venodilation in all rats (Fig. 5A). SBV was reduced by 3 to 35% ($p < 0.001$) of the postinfarction value. On average, SVR was also reduced ($p = 0.003$). However, neither HR nor E_n increased to counteract this loss, resulting in a significant drop in MAP ($p < 0.001$). Instead, HR remained steady and the average E_n decreased slightly ($p = 0.54$ and $p = 0.02$, respectively). We computed the correlation coefficients between the changes in each pair of compensatory mechanisms to quantify their interactions and no relationships were significant. The reductions in MAP and MAP induced by nitroglycerin were significantly correlated however, implicating venodilation as the primary mechanism driving the observed reduction in mean arterial pressure (Supplemental Fig. 4).

As anticipated, following the postinfarction administration of dobutamine there was increased contractility in the surviving myocardium of all rats (Fig. 5B). E_n increased by 12 to 300% ($p = 0.002$) of the postinfarction value. On average, HR showed a slight, but statistically significant increase ranging from 0 to 7% ($p < 0.001$). There was also a small but significant increase in average MAP ($p = 0.03$). Again, we computed the correlation coefficients between the changes in each pair of compensatory mechanisms and no relationships were significant.

Next, we plotted the change in each compensatory mechanism with pharmacologic perturbation as a function of its initial postinfarction value. We anticipated that the rats who increased venoconstriction the most in response to MI would exhibit the largest levels of venodilation with nitroglycerin administration. However, there was no correlation between the change in stressed blood volume postinfarction and its further alteration with nitroglycerin (Fig. 6A), indicating nitroglycerin had similar venodilatory effects regardless of the levels of venoconstriction immediately following MI. By contrast, there was a

significant relationship between the degree of venoconstriction (change in stressed blood volume) post-infarction and the effect of nitroglycerin on mean arterial pressure (Fig. 6B). Animals with limited venoconstriction in response to MI showed large drops in blood pressure with nitroglycerin, while animals with strong venoconstriction responses experienced smaller drops in MAP. The physiologic and therapeutic implications of this finding require further study.

We also anticipated that individual rats who increased myocardial contractility the most in response to MI would exhibit the smallest increases in contractility when dobutamine was administered. However, there was no correlation between the postinfarction end-systolic elastance of the surviving myocardium and its further alteration with dobutamine (Fig. 6C).

3.3. Hypertrophic mechanical stimuli

Next, we considered how infarction and subsequent pharmacologic treatment would affect the patterns of post-infarction remodeling according to an established model of mechanically-driven hypertrophy that correctly predicted patterns of ventricular hypertrophy following pressure overload (aortic banding), volume overload (mitral valve damage), and myocardial infarction (coronary artery ligation) [21,25]. In that model, an increase in peak λ_c is associated with eccentric hypertrophy and left ventricular dilation, while changes in peak λ_r are associated with wall thinning or thickening. Stretches were computed for the noninfarcted region of left ventricle only. Peak λ_c increased on average following myocardial infarction (Fig. 7A). In prior modeling studies, the difference in peak λ_c required to trigger eccentric hypertrophy was ~0.1 [21,25]. Assuming this level is applicable to rats, we would expect 6 of the 13 rats studied here to exhibit ventricular dilation post-infarction. Both dobutamine and nitroglycerin significantly reduced peak λ_c post-infarction, with nitroglycerin restoring peak λ_c to control levels (Fig. 7B). Thus, current models would predict that either agent should reduce the risk of eccentric hypertrophy and left ventricular dilation. On average, peak λ_r did not increase or decrease postinfarction (Fig. 7C). Thus, on average, we would not expect significant thickening or thinning of the noninfarcted myocardium with MI. Both dobutamine and nitroglycerin significantly reduced peak λ_r post-infarction (Fig. 7D).

Next, we quantified the relationship between hemodynamic compensation and peak λ_c and λ_r of the noninfarcted myocardium. On average, there was a significant positive correlation between stressed blood volume and peak λ_c difference postinfarction (Fig. 8A). There were also significant correlations between both stressed blood volume and end-systolic elastance of the surviving myocardium and peak λ_r difference postinfarction (Fig. 8B and C). Infarct size is weakly correlated with eccentric hypertrophy [12,13] in patients and less so in rats [52,53]. In our study, neither the difference in peak λ_c nor the difference in peak λ_r post infarction were significantly correlated with infarct size (Supplemental Fig. 5).

4. Discussion

The goal of this study was quantify the variability and interdependence of post-infarction reflex compensatory mechanisms with and without pharmacologic perturbation. There are

three novel aspects of this study relative to prior work. First, we collected rat-specific hemodynamic data both before and after coronary artery ligation and with various pharmacologic agents. By applying our previously published modeling approach [21] to these paired measurements, we were able to quantify relationships between reflex mechanisms and more rigorously test the hypothesis that postinfarction compensation is highly variable. Second, we perturbed compensation with pharmacologic agents to test whether the balance of reflex mechanisms employed by individual animals could predict responses to pharmacologic perturbation. Third, using an established model of cardiac remodeling we computed stretch in the surviving myocardium and examined how predicted ventricular hypertrophy was influenced by both reflex compensation and administration of drugs. Together, the methods and results presented here suggest that there is a high degree of variability in the mixture of reflex compensation employed by individual animals post-infarction, use of venoconstriction increases peak circumferential stretch in the myocardium and predicted ventricular enlargement post-infarction, and that customizing pharmacologic therapy to individuals based on their initial response to infarction will be challenging because initial response was a poor predictor of subsequent response to pharmacologic agents.

4.1. Compensation

Using a computational model, we were able to estimate the compensatory balance in rats postinfarction, postinfarction with dobutamine, and postinfarction with nitroglycerin. The model parameters reflecting myocardial contractility and venoconstriction, which cannot be measured directly in infarcted animals, were fitted by minimizing the sum squared error in the left ventricular end-diastolic and end-systolic volumes with a high level of accuracy (maximum error was <1%). Consistent with our previous findings [21], the mix of mechanisms employed by individual animals for post-infarction compensation was highly variable (Fig. 3). Changes in heart rate were least variable among the mechanisms examined, which may be in part a result of the use of a rodent model. While other studies have reported similar [54,55] or slightly higher [56,57] levels of variability in heart rate post-infarction in rats, none reached the levels observed in dogs [21]. Additionally, in studies that reported both post-infarction heart rate and arterial resistance changes in rats, variability was about 2-fold higher in arterial resistance [56,57]. These differences are consistent with broader observations that smaller mammals have reduced capacity to increase heart rate [58]. Postinfarction variability in mean arterial pressure was consistent with previous studies [54,56,57,59]. In most of these studies, a significant reduction in mean arterial pressure was observed, however they purposely considered larger infarcts (average sizes of 40 to 50%).

We were able to detect a significant negative relationship between myocardial contractility and venoconstriction because we tracked postinfarction compensation in individual animals (Fig. 4). However, when myocardial contractility was increased by dobutamine, venoconstriction was unchanged (Fig. 5B). Additionally, when venodilation was induced by nitroglycerin, myocardial contractility was reduced (Fig. 5A). Thus, the inverse relationship between myocardial contractility and venoconstriction was not sustained in the presence of pharmacologic agents. Instead, dobutamine and nitroglycerin had significant effects on mean arterial pressure itself. We observed a slight but significant average increase in

both mean arterial pressure and heart rate with dobutamine administration. Nitroglycerin significantly and substantially reduced mean arterial pressure along with arterial resistance and myocardial contractility. We purposely administered low doses of both dobutamine (4 μg/kg) and nitroglycerin (20 μg/kg) to discern their effects on compensation. For comparison, the dose of dobutamine for rats during standard stress testing ranges from about 10 to 20 μg/kg [29,60,61] and can reach 100 μg/kg [30], corresponding to average increases in heart rate of 15 to 25% and up to 50%. However, even at these low doses, individual animals did not exhibit the responses we would have predicted based on their initial post-infarction reflex response; therefore, customizing pharmacologic therapy to individuals to account for variability in reflex responses would appear to be challenging.

4.2. Hypertrophic mechanical stimuli

Cardiomyocytes grow and remodel in response to changes in their mechanical environment. Even in the absence of neurohormonal factors, physical stretching of cardiomyocytes has been shown to induce a hypertrophic response [62]. In previous studies, potential hypertrophic mechanical stimuli have been quantified both experimentally [22,23,40] and computationally [24,26] based on their ability to produce classic patterns of concentric and eccentric ventricular hypertrophy following pressure and volume overloading, respectively. Computational models utilizing these stimuli have also been successful at predicting hypertrophic patterns in dogs following myocardial infarction [21,25] and left bundle branch block [63]. In our previously published model capable of predicting ventricular dimensions in dogs post-infarction, increases in peak λ_c lead to ventricular enlargement and increases in peak λ_r lead to ventricular thickening [21,25]. Within this study, we used a computational model to compute these stretches within the noninfarcted region of the left ventricle. On average, peak λ_c increased and peak λ_r was not significantly different postinfarction. Based on these our results,we would expect left ventircular dilation in six rats. There was a significant positive relationship between stressed blood volume and peak λ_c, indicating venoconstriction as a risk factor for post-infarction ventricular remodeling and dilation. However, this relationship was modulated by the other compensatory mechanisms. For example, while the rats shown in lilac and hot pink exhibited similar levels of venoconstriction (Fig. 3), the peak λ_c difference postinfarction was much lower for the hot pink rat due to postinfarction arterial dilation and a drop in mean arterial pressure, which mitigated the effects of venoconstriction. Thus, a complete description of hemodynamic compensation is likely needed to produce accurate predictive computational models for individuals. Stressed blood volume and end-systolic elastance of the noninfarct compartment were also significantly correlated with peak λ_r difference postinfarction. In prior modeling studies, however, the difference in peak λ_r necessary to trigger thinning or thickening was about − 0.3 and 0.3, respectively, indicating this relationship was inconsequential. Dobutamine and nitroglycerin significantly reduced both peak λ_c and λ_r. For the purposes of this study, we focused on dobutamine and nitroglycerin because their high clearance rates enabled us to measure their effects on postinfarction compensation in succession in each rat, but as we consider the implications of compensation on ventricular hypertrophy and heart failure, other chronic pharmacologic agents will be needed.

4.3. Infarct region

Within our analysis, we assumed that the infarct region was no longer contractile and that its passive properties were unchanged. This is a reasonable assumption for the timescale of our experiment. Chronically, however, the changing composition, structure, and mechanical properties of the healing infarct scar all affect ventricular function (see review in [64]). Thus, hypertrophy of the noninfarcted region and remodeling of the infarct scar are intrinsically coupled. Acutely, within hours, infarcted muscle undergoes necrosis, the collagenase activity of matrix metalloproteinases (MMPs) increases, and the activity of various pro-inflammatory and pro-fibrotic cytokines increases. The degree of individual variability in these processes has received relatively little attention. While there is ample evidence that hours postinfarction IL-6, IL-1β, TNFα and TGFβ as well as MMP8 and MMP9 increase dramatically in the infarct region [55,65–68], few studies quantify variability. Interestingly in two of these studies [55,69], myocardial infarction increased the coefficient of variation in mRNA expression in IL-6 and IL- 1β, but actually decreased the coefficient of variation in MMP8 and MMP9. Reperfusion therapy likely alters both the increase in cytokines and MMPs as well as their variability [68,70].

4.4. Limitations and sources of error

We measured hemodynamics in anesthetized, open-chest rats. Isoflurane anesthesia is known to offer some protection from myocardial ischemia; however, since we were not attempting to achieve a specific infarct size in this study and the dose and ligation sites were standardized, any effects on infarct size were not critical to interpreting our results. By contrast, isoflurane is also known to induce vasodilation [71], which could have changed the degree to which the animals we studied compensated for MI with arterial or venous vasoconstriction, compared to what would have been observed in conscious animals. We chose isoflurane because multiple studies reported less cardiac depression and reduction of heart rate in rodents with isoflurane compared to other anesthetics [72]. We found a single study suggesting that isoflurane slightly increased day-to-day variability in measured blood pressures [73], but no other data suggesting that the reflex variability among individual animals reported here was primarily due to our choice of anesthetic. This interpretation is supported by the fact that our prior finding of high variability in post-infarction reflex responses was based on data from dogs anesthetized with a different agent (pentobarbital) [21].

A potential technical source of error in this study was the ability to place sonomicrometers accurately at selected landmarks on the beating in situ left ventricle. Inaccurate placement of the sonomicrometers would produce a random multiplicative error in calculated ventricular volumes. To avoid these errors we imaged sonomicrometer placement on the ventricle in situ and following arrest. Segment lengths were corrected assuming homogeneous deformation along the major axes of the heart. Another potential technical source of error was drift or offset in the Millar miniature pressure transducer. The transducer calibration slope was stable across all studies, but the offset varied. Offset was removed assuming minimum left ventricular pressure in an open-chest rat should be approximately zero [22]. Due to the expected variability in postinfarction compensation, it was critical to perform acute measurements at multiple time points and pharmacologic states longitudinally in each

animal. However, this increased the complexity and time required for the surgical procedures performed, likely leading to our somewhat high exclusion rate of 41%.

We fit hemodynamic compensatory reflex profiles in individual rats following myocardial infarction using our previously published compartmental model of the heart coupled to a circuit model of the circulation [21,25]. The simplicity of this model was key for animal-specific simulation and fitting since it runs in just seconds on a desktop computer. Therefore, the automated algorithms used to fit end- systolic elastance of the surviving myocardium and stress blood volume required just minutes for each rat. To simulate infarction we divided the damaged left ventricle into a noninfarcted, contractile compartment, and an infarcted, non-contractile compartment. Sunagawa et al. [74] showed that this simple approach replicates measured pressure–volume behavior across a wide range of infarct sizes and Li et al. [75] extended the approach to model regional ischemia. When modeling cardiac growth and remodeling, a geometric model of the left ventricle is necessary to compute stresses and stretches. An advantage of finite element models is that they can more faithfully represent geometries derived from high-resolution imaging such as MRI or CT. However, the time required to both construct and run these models makes them impractical for animal-specific simulation. To compute growth stimuli we followed our previous approach [21,25] and assumed a thin-walled spherical geometry. In the past, this limitation did not impair our ability to predict relative changes in radius and wall thickness. We believe that the spherical geometry was successful because alterations in ventricular pressure and volume have similar relative impacts on stress as in geometries that are more complex. Multi-compartmental approaches have also been successfully used by others [76,77] to reproduce aspects of left ventricular dyssynchrony and resynchronization therapy.

Given the terminal nature of our study, we were unable to measure ventricular dimensions chronically following myocardial infarction. Therefore, we could not test animal-specific predictions of eccentric hypertrophy. Key to testing these types of rat-specific predictions are less invasive techniques for measuring hemodynamics. We utilized sonomicrometry in this acute study since it enabled rapid measurement of ventricular volumes simultaneously with invasive ventricular pressures. Ultrasound or magnetic resonance imaging capture much higher resolutions and provide better estimations of ventricular dimensions and shape [78,79]. These techniques are also noninvasive, making them ideal for longitudinal studies. Mean arterial pressure has also been measured longitudinally in rats using radiotelemetry and tail-cuff methods over periods of many weeks [80–82]. Unfortunately, noninvasive ventricular pressure measurement is challenging in small animals, and for any future chronic study aiming to test the predictive power of our modeling approach chronic measurement of left ventricular pressures will be essential.

5. Conclusion

The experimental data and model simulations presented here confirm that there is substantial individual variability in hemodynamic compensation postinfarction. Postinfarction compensation did affect subsequent pharmacologic perturbation of these mechanisms, but not as expected. On average, there were significant average changes in mean arterial pressure with both dobutamine and nitroglycerin administration rather than a rebalancing of

compensation. Initial levels of venoconstriction did modulate the tendency of nitroglycerin to cause hypotension, however, potentially indicating a means to stratify individuals for venodilators. Ventricular hypertrophy and left ventricular dilation were predicted for about half of the rats in our study based on previous studies relating stretch to hypertrophy. Low doses of dobutamine and nitroglycerin reduced this risk, suggesting that early modulation of ventricular mechanics could reduce ventricular hypertrophy and failure. However, the fact that initial reflex responses to infarction were a poor predictor of subsequent responses to pharmacologic agents suggests that customizing pharmacologic therapy to individuals based on an initial acute response to MI will be challenging.

Supplementary Material

Refer to Web version on PubMed Central for supplementary material.

Funding

This work was supported by the National Institutes of Health (U01 HL127654; Funder ID: 10.13039/100000002) and the American Heart Association (17 POST 33660943; Funder ID: 10.13039/100000968).

References

[1]. Aparicio HJ, Benjamin EJ, Callaway CW, Carson AP, Cheng S, Elkind MSV, Evenson KR, Ferguson JF, Knutson KL, Lee CD, Lewis TT, Loop MS, Lutsey P, Mackey J, Matchar DB, Heart Disease and Stroke Statistics-2021 Update A Report from the American Heart Association, 2021, 10.1161/CIR.0000000000000950.

[2]. Benjamin EJ, Virani SS, Callaway CW, Chamberlain AM, Chang AR, Cheng S, Chiuve SE, Cushman M, Delling FN, Deo R, de Ferranti SD, Ferguson JF, Fornage M, Gillespie C, Isasi CR, Jimenez MC´, Jordan LC, Judd SE, Lackland D, Lichtman JH, Lisabeth L, Liu S, Longenecker CT, Lutsey PL, Mackey JS, Matchar DB, Matsushita K, Mussolino ME, Nasir K, O'Flaherty M, Palaniappan LP, Pandey A, Pandey DK, Reeves MJ, Ritchey MD, Rodriguez CJ, Roth GA, Rosamond WD, Sampson UKA, Satou GM, Shah SH, Spartano NL, Tirschwell DL, Tsao CW, Voeks JH, Willey JZ, Wilkins JT, Wu JHY, Alger HM, Wong SS, Muntner P, Heart Disease and Stroke Statistics—2018 Update: A Report From the American Heart Association, Circulation 137 (2018), 10.1161/CIR.0000000000000558. E67–E492. [PubMed: 29386200]

[3]. Bahit MC, Kochar A, Granger CB, Post-Myocardial Infarction Heart Failure, JACC Hear. Fail 6 (2018) 201–208, 10.1016/j.jchf.2017.09.015.

[4]. Chen J, Hsieh AFC, Dharmarajan K, Masoudi FA, Krumholz HM, National trends in heart failure hospitalization after acute myocardial infarction for medicare beneficiaries 1998–2010, Circulation. 128 (2013) 2577–2584, 10.1161/CIRCULATIONAHA.113.003668. [PubMed: 24190958]

[5]. Luca Salvagno G, Pavan C, Prognostic biomarkers in acute coronary syndrome, Ann. Transl. Med 4 (2016) 1–8, 10.21037/atm.2016.06.36.

[6]. Cahill TJ, Kharbanda RK, Heart failure after myocardial infarction in the era of primary percutaneous coronary intervention: Mechanisms, incidence and identification of patients at risk, World J. Cardiol 9 (2017) 407, 10.4330/wjc.v9.i5.407. [PubMed: 28603587]

[7]. Clerfond G, Bière L, Mateus V, Grall S, Willoteaux S, Prunier F, Furber A, End-systolic wall stress predicts post-discharge heart failure after acute myocardial infarction MOTS CLES, Arch. Cardiovasc. Dis 108 (2015) 310–320, 10.1016/j.acvd.2015.01.008. [PubMed: 25858536]

[8]. White HD, Norris RM, Brown MA, Brandt PW, Whitlock RM, Wild CJ, Left ventricular end-systolic volume as the major determinant of survival after recovery from myocardial infarction, Circulation. 76 (1987) 44–51, 10.1161/01.CIR.76.1.44. [PubMed: 3594774]

[9]. Jenča D, Melenovský V, Stehlik J, Stanek V, Kettner J, Kautzner J, Adámková V, Wohlfahrt P, Heart failure after myocardial infarction: incidence and predictors, ESC Hear. Fail 8 (2021) 222–237, 10.1002/ehf2.13144.

[10]. Ponikowski P, Anker SD, AlHabib KF, Cowie MR, Force TL, Hu S, Jaarsma T, Krum H, Rastogi V, Rohde LE, Samal UC, Shimokawa H, Budi Siswanto B, Sliwa K, Filippatos G, Heart failure: preventing disease and death worldwide, ESC Hear. Fail 1 (2014) 4–25, 10.1002/ehf2.12005.

[11]. Schocken DD, Benjamin EJ, Fonarow GC, Krumholz HM, Levy D, Mensah GA, Narula J, Shor ES, Young JB, Hong Y, Prevention of heart failure: A scientific statement from the American Heart Association Councils on epidemiology and prevention, clinical cardiology, cardiovascular nursing, and high blood pressure research; Quality of Care and Outcomes Research Interdisc, Circulation. 117 (2008) 2544–2565, 10.1161/CIRCULATIONAHA.107.188965. [PubMed: 18391114]

[12]. Bulluck H, Go YY, Crimi G, Ludman AJ, Rosmini S, Abdel-Gadir A, Bhuva AN, Treibel TA, Fontana M, Pica S, Raineri C, Sirker A, Herrey AS, Manisty C, Groves A, Moon JC, Hausenloy DJ, Defining left ventricular remodeling following acute ST-segment elevation myocardial infarction using cardiovascular magnetic resonance, J. Cardiovasc. Magn. Reson 19 (2017) 1–13, 10.1186/s12968-017-0343-9. [PubMed: 28081721]

[13]. Wu E, Ortiz JT, Tejedor P, Lee DC, Bucciarelli-Ducci C, Kansal P, Carr JC, Holly TA, Lloyd-Jones D, Klocke FJ, Bonow RO, Infarct size by contrast enhanced cardiac magnetic resonance is a stronger predictor of outcomes than left ventricular ejection fraction or end-systolic volume index: prospective cohort study, Heart 94 (2008) 730–736, 10.1136/hrt.2007.122622. [PubMed: 18070953]

[14]. Francis GS, McDonald KM, Cohn JN, Neurohumoral activation in preclinical heart failure. Remodeling and the potential for intervention, Circulation 87 (1993). IV90–6. http://www.ncbi.nlm.nih.gov/pubmed/8097970.

[15]. Hartupee J, Mann DL, Neurohormonal activation in heart failure with reduced ejection fraction, Nat. Rev. Cardiol 14 (2017) 30–38, 10.1038/nrcardio.2016.163. [PubMed: 27708278]

[16]. Campos LA, Bader M, Baltatu OC, Brain renin-angiotensin system in hypertension, cardiac hypertrophy, and heart failure, Front. Physiol 2 (JAN) (2012) 1–5, 10.3389/fphys.2011.00115.

[17]. Chiladakis JA, Patsouras N, Manolis AS, The Bezold-Jarisch reflex in acute inferior myocardial infarction: Clinical and sympathovagal spectral correlates, Clin. Cardiol 26 (2003) 323–328, 10.1002/clc.4950260706. [PubMed: 12862298]

[18]. Wei JY, Markis JE, Malagold M, Braunwald E, Cardiovascular reflexes stimulated by reperfusion of ischemic myocardium in acute myocardial infarction, Circulation. 67 (1983) 796–801, 10.1161/01.CIR.67.4.796. [PubMed: 6825235]

[19]. Rothe CF, Reflex control of veins and vascular capacitance, Physiol. Rev 63 (1983) 1281–1342, 10.1152/physrev.1983.63.4.1281. [PubMed: 6361810]

[20]. Miller WL, Fluid volume overload and congestion in heart failure, Circ. Heart Fail 9 (2016) 1–9, 10.1161/CIRCHEARTFAILURE.115.002922.

[21]. Witzenburg CM, Holmes JW, The Impact of Hemodynamic Reflex Compensation Following Myocardial Infarction on Subsequent Ventricular Remodeling, J. Biomech. Eng 141 (2019), 10.1115/1.4043867.

[22]. Holmes JW, Candidate mechanical stimuli for hypertrophy during volume overload, J. Appl. Physiol 97 (2004) 1453–1460, 10.1152/japplphysiol.00834.2003. [PubMed: 15169750]

[23]. Emery JL, Omens JH, Mechanical regulation of myocardial growth during volume-overload hypertrophy in the rat, Am. J. Phys 273 (1997) H1198–H1204, http://www.ncbi.nlm.nih.gov/pubmed/9321807.

[24]. Witzenburg CM, Holmes JW, A Comparison of Phenomenologic Growth Laws for Myocardial Hypertrophy, J. Elast 129 (2017) 257–281, 10.1007/s10659-017-9631-8. [PubMed: 29632418]

[25]. Witzenburg CM, Holmes JW, Predicting the Time Course of Ventricular Dilation and Thickening Using a Rapid Compartmental Model, J. Cardiovasc. Transl. Res 11 (2018) 109–122, 10.1007/s12265-018-9793-1. [PubMed: 29550925]

[26]. Rondanina E, Bovendeerd PHM, Stimulus–effect relations for left ventricular growth obtained with a simple multi-scale model: the influence of hemodynamic feedback, Biomech. Model. Mechanobiol 19 (2020) 2111–2126, 10.1007/s10237-020-01327-2. [PubMed: 32358671]

[27]. Fomovsky GM, Holmes JW, Evolution of scar structure, mechanics, and ventricular function after myocardial infarction in the rat, AJP Hear. Circ. Physiol 298 (2010) H221–H228, 10.1152/ajpheart.00495.2009.

[28]. Fishbein MC, Maclean D, Maroko PR, Experimental myocardial infarction in the rat; qualitative and quantitative changes during pathological evolution, Am. J. Pathol 90 (1978) 57–70. [PubMed: 619696]

[29]. Sasaki H, Fukuda S, Otani H, Zhu L, Yamaura G, Engelman RM, Das DK, Maulik N, Hypoxic preconditioning triggers myocardial angiogenesis: a novel approach to enhance contractile functional reserve in rat with myocardial infarction, J. Mol. Cell. Cardiol 34 (2002) 335–348, 10.1006/jmcc.2001.1516. [PubMed: 11945025]

[30]. Stehlin E, Malpas SC, Budgett DM, Barrett CJ, McCormick D, Whalley G, Fu F, Beil M, Rigel DF, Guild S-J, Chronic measurement of left ventricular pressure in freely moving rats, J. Appl. Physiol 115 (2013) 1672–1682, 10.1152/japplphysiol.00683.2013. [PubMed: 24114699]

[31]. Miller RR, Vismara LA, Williams DO, Amsterdam EA, Mason DT, Pharmacological mechanisms for left ventricular unloading in clinical congestive heart failure. Differential effects of nitroprusside, phentolamine, and nitroglycerin on cardiac function and peripheral circulation, Circ. Res 39 (1976) 127–133, 10.1161/01.RES.39.1.127. [PubMed: 819179]

[32]. Bauer JA, Fung HL, Arterial versus venous metabolism of nitroglycerin to nitric oxide: a possible explanation of organic nitrate venoselectivity, J. Cardiovasc. Pharmacol 28 (1996) 371–374, http://www.ncbi.nlm.nih.gov/pubmed/8877582. [PubMed: 8877582]

[33]. Bassenge E, Zanzinger J, Nitrates in different vascular beds, nitrate tolerance, and interactions with endothelial function, Am. J. Cardiol 70 (1992) B23–B29, 10.1016/0002-9149(92)90591-L.

[34]. Ogilvie RI, Effect of nitroglycerin on peripheral blood flow distribution and venous return, J. Pharmacol. Exp. Ther 207 (1978) 372–380, http://www.ncbi.nlm.nih.gov/pubmed/101653. [PubMed: 101653]

[35]. Fomovsky GM, Holmes JW, Evolution of scar structure, mechanics, and ventricular function after myocardial infarction in the rat, AJP Hear. Circ. Physiol 298 (2010) H221–H228, 10.1152/ajpheart.00495.2009.

[36]. Hale SL, Vivaldi MT, Kloner RA, Fluorescent microspheres: a new tool for visualization of ischemic myocardium in rats, Am. J. Phys 251 (1986) H863–H868, 10.1152/ajpheart.1986.251.4.H863.

[37]. Allen TH, Krzywicki HJ, Roberts JE, Density, fat, water and solids in freshly isolated tissues, J. Appl. Physiol 14 (1959) 1005–1008, 10.1152/jappl.1959.14.6.1005. [PubMed: 13792786]

[38]. Yipintsoi T, Scanlon PD, Bassingthwaighte JB, Density and Water Content of Dog Ventricular Myocardium, Exp. Biol. Med 141 (1972) 1032–1035, 10.3181/00379727-141-36927.

[39]. Suga H, Sagawa K, Shoukas AA, Load independence of the instantaneous pressure-volume ratio of the canine left ventricle and effects of epinephrine and heart rate on the ratio, Circ. Res 32 (1973) 314–322, 10.1161/01.RES.32.3.314. [PubMed: 4691336]

[40]. Grossman W, Braunwald E, Mann T, McLaurin LP, Green LH, Contractile state of the left ventricle in man as evaluated from end-systolic pressure-volume relations, Circulation. 56 (1977) 845–852, 10.1161/01.CIR.56.5.845. [PubMed: 71960]

[41]. Kass DA, Maughan WL, From “Emax” to pressure-volume relations: A broader view, Circulation. 77 (1988) 1203–1212, 10.1161/01.CIR.77.6.1203. [PubMed: 3286035]

[42]. Bogen DK, Rabinowitz SA, Needleman A, McMahon TA, Abelmann WH, An analysis of the mechanical disadvantage of myocardial infarction in the canine left ventricle, Circ. Res 47 (1980) 728–741, 10.1161/01.RES.47.5.728. [PubMed: 7418131]

[43]. Sunagawa K, Maughan WL, Sagawa K, Effect of regional ischemia on the left ventricular end-systolic pressure-volume relationship of isolated canine hearts, Circ. Res 52 (1983), 170 LP–178, http://circres.ahajournals.org/content/52/2/170.abstract. [PubMed: 6825214]

[44]. Witzenburg CM, Holmes JW, Predicting the Time Course of Ventricular Dilation and Thickening Using a Rapid Compartmental Model, J. Cardiovasc. Transl. Res 11 (2018) 109–122, 10.1007/s12265-018-9793-1. [PubMed: 29550925]

[45]. West GB, Brown JH, Enquist BJ, A general model for the origin of allometric scaling laws in biology, Science (80-.) 276 (1997) 122–126, 10.1126/science.276.5309.122.

[46]. Seymour RS, Blaylock AJ, The principle of laplace and scaling of ventricular wall stress and blood pressure in mammals and birds, Physiol. Biochem. Zool 73 (2000) 389–405, 10.1086/317741. [PubMed: 11009393]

[47]. Lindstedt SL, Schaeffer PJ, Use of allometry in predicting anatomical and physiological parameters of mammals, Lab. Anim 36 (2002) 1–19, 10.1258/0023677021911731. [PubMed: 11833526]

[48]. Baretta A, Corsini C, Yang W, Vignon-Clementel IE, Marsden AL, Feinstein JA, Hsia TY, Dubini G, Migliavacca F, Pennati G, Virtual surgeries in patients with congenital heart disease: A multi-scale modelling test case, Philos. Trans. <tr>R. Soc</tr>. A Math. Phys. Eng. Sci 369 (2011) 4316–4330, 10.1098/rsta.2011.0130.

[49]. Westerhof N, Elzinga G, Normalized input impedance and arterial decay time over heart period are independent of animal size, Am. J. Phys. Regul. Integr. Comp. Phys 261 (1991), 10.1152/ajpregu.1991.261.1.r126.

[50]. Magder S, De Varennes B, Clinical death and the measurement of stressed vascular volume, Crit. Care Med 26 (1998) 1061–1064, http://www.ncbi.nlm.nih.gov/pubmed/9635656. [PubMed: 9635656]

[51]. Gelman S, Venous function and central venous pressure: a physiologic story, Anesthesiology. 108 (2008) 735–748, 10.1097/ALN.0b013e3181672607. [PubMed: 18362606]

[52]. Minicucci MF, Azevedo PS, Ardisson LP, Okoshi K, Matsubara BB, Matsubara LS, Paiva SAR, Zornoff LAM, Relevance of the ventricular remodeling pattern in the model of myocardial infarction in rats, Arq. Bras. Cardiol 95 (2010) 635–639, 10.1590/S0066-782X2010005000130. [PubMed: 20857043]

[53]. Pfeffer MA, Braunwald E, Ventricular Remodeling After Myocardial Infarction Experimental Observations and Clinical Implications, Circulation. 81 (1989) 1161–1172.

[54]. Hama N, Itoh H, Shirakami G, Nakagawa O, Suga S, Ogawa Y, Masuda I, Nakanishi K, Yoshimasa T, Hashimoto Y, Yamaguchi M, Hori R, Yasue H, Nakao K, Rapid Ventricular Induction of Brain Natriuretic Peptide Gene Expression in Experimental Acute Myocardial Infarction, Circulation. 92 (1995) 1558–1564, 10.1161/01.CIR.92.6.1558. [PubMed: 7664440]

[55]. González GE, Rabald S, Briest W, Gelpi RJ, Seropian I, Zimmer HG, Deten A, Ribose treatment reduced the infarct size and improved heart function after Myocardial Infarction in rats, Cell. Physiol. Biochem 24 (2009) 211–218, 10.1159/000233247. [PubMed: 19710536]

[56]. Drexler H, Toggart EJ, Glick MR, Heald J, Flaim SF, Zelis R, Regional vascular adjustments during recovery from myocardial infarction in rats, J. Am. Coll. Cardiol 8 (1986) 134–142, 10.1016/S0735-1097(86)80104-8. [PubMed: 3711508]

[57]. Sandmann S, Bohle RM, Dreyer T, Unger T, The T-type calcium channel blocker mibefradil reduced interstitial and perivascular fibrosis and improved hemodynamic parameters in myocardial infarction-induced cardiac failure in rats, Virchows Arch. 436 (2000) 147–157, 10.1007/PL00008215. [PubMed: 10755606]

[58]. Milani-Nejad N, Janssen PML, Small and large animal models in cardiac contraction research: Advantages and disadvantages, Pharmacol. Ther 141 (2014) 235–249, 10.1016/j.pharmthera.2013.10.007. [PubMed: 24140081]

[59]. Matsumoto-Ida M, Takimoto Y, Aoyama T, Akao M, Takeda T, Kita T, Activation of TGF-β1-TAK1-p38 MAPK pathway in spared cardiomyocytes is involved in left ventricular remodeling after myocardial infarction in rats, Am. J. Physiol. Circ. Physiol 290 (2006) H709–H715, 10.1152/ajpheart.00186.2005.

[60]. Fukuda S, Kaga S, Sasaki H, Zhan L, Zhu L, Otani H, Kalfin R, Das DK, Maulik N, Angiogenic signal triggered by ischemic stress induces myocardial repair in rat during chronic infarction, J. Mol. Cell. Cardiol 36 (2004) 547–559, 10.1016/j.yjmcc.2004.02.002. [PubMed: 15081314]

[61]. Plante E, Lachance D, Drolet MC, Roussel É, Couet J, Arsenault M, Dobutamine stress echocardiography in healthy adult male rats, Cardiovasc. Ultrasound 3 (2005) 1–7, 10.1186/1476-7120-3-34. [PubMed: 15655075]

[62]. Sadoshima J, Izumo S, The Cellular and Molecular Response of Cardiac Myocytes, Annu. Rev. Physiol (1997) 551–571. [PubMed: 9074777]

[63]. Kerckhoffs RCP, Omens JH, McCulloch AD, Mulligan LJ, Ventricular dilation and electrical dyssynchrony synergistically increase regional mechanical nonuniformity but not mechanical dyssynchrony: a computational model, Circ. Heart Fail 3 (2010) 528–536, 10.1161/CIRCHEARTFAILURE.109.862144. [PubMed: 20466849]

[64]. Holmes JW, Borg TK, Covell JW, Structure and mechanics of healing myocardial infarcts, Annu. Rev. Biomed. Eng 7 (2005) 223–253, 10.1146/annurev.bioeng.7.060804.100453. [PubMed: 16004571]

[65]. Deten A, Zimmer HG, Heart function and cytokine expression is similar in mice and rats after myocardial infarction but differences occur in TNFα expression, Pflugers Arch. - Eur. J. Physiol 445 (2002) 289–296, 10.1007/s00424-002-0930-x. [PubMed: 12457250]

[66]. Deten A, Volz HC, Driest W, Zimmer HG, Cardiac cytokine expression is upregulated in the acute phase after myocardial infarction, Experimental studies in rats, Cardiovasc. Res 55 (2002) 329–340, 10.1016/S0008-6363(02)00413-3. [PubMed: 12123772]

[67]. Deten A, Volz HC, Briest W, Zimmer HG, Differential cytokine expression in myocytes and non-myocytes after myocardial infarction in rats, Mol. Cell. Biochem 242 (2003) 47–55, 10.1023/A:1021129410221. [PubMed: 12619865]

[68]. Herskowitz A, Choi S, Ansari AA, Wesselingh S, Cytokine mRNA expression in postischemic/reperfused myocardium, Am. J. Pathol 146 (1995) 419–428. [PubMed: 7856752]

[69]. Herzog E, Gu A, Kohmoto T, Burkhoff D, Hochman JS, Early Activation of Metalloproteinases after Experimental Myocardial Infarction Occurs in Infarct and Non-infarct Zones, Cardiovasc. Pathol 7 (1998) 307–312, 10.1016/S1054-8807(98)00008-8. [PubMed: 25851597]

[70]. Carlyle WC, Jacobson AW, Judd DL, Tian B, Chu C, Hauer KM, Hartman MM, McDonald KM, Delayed reperfusion alters matrix metalloproteinase activity and fibronectin mRNA expression in the infarct zone of the ligated rat heart, J. Mol. Cell. Cardiol 29 (1997) 2451–2463, 10.1006/jmcc.1997.0482. [PubMed: 9299368]

[71]. Munting LP, Derieppe MPP, Suidgeest E, Denis de Senneville B, Wells JA, van der Weerd L, Influence of different isoflurane anesthesia protocols on murine cerebral hemodynamics measured with pseudo-continuous arterial spin labeling, NMR Biomed. 32 (2019) 1–12, 10.1002/nbm.4105.

[72]. Sano Y, Ito S, Yoneda M, Nagasawa K, Matsuura N, Yamada Y, Uchinaka A, Bando YK, Murohara T, Nagata K, Effects of various types of anesthesia on hemodynamics, cardiac function, and glucose and lipid metabolism in rats, Am. J. Physiol. Heart Circ. Physiol 311 (2016) H1360–H1366, 10.1152/ajpheart.00181.2016.

[73]. Hem NA, Phie J, Chilton L, Kinobe R, A volume-pressure tail cuff method for hemodynamic parameters: Comparison of restraint and light isoflurane anesthesia in normotensive male Lewis rats, J. Pharmacol. Toxicol. Methods 100 (2019) 106601, 10.1016/j.vascn.2019.106601.

[74]. Sunagawa K, Maughan WL, Sagawa K, Effect of regional ischemia on the left ventricular end-systolic pressure-volume relationship of isolated canine hearts, Circ. Res 52 (1983) 170–178, http://www.ncbi.nlm.nih.gov/pubmed/6825214. [PubMed: 6825214]

[75]. Li JK, Wang J, Drzewiecki G, Computer modeling of non-adjacent regional ischemic zones on ventricular function, Comput. Biol. Med 26 (1996) 371–383, 10.1016/0010-4825(96)00025-X. [PubMed: 8889335]

[76]. Walmsley J, Arts T, Derval N, Bordachar P, Cochet H, Ploux S, Prinzen FW, Delhaas T, Lumens J, Fast Simulation of Mechanical Heterogeneity in the Electrically Asynchronous Heart Using the MultiPatch Module, PLoS Comput. Biol 11 (2015), e1004284, 10.1371/journal.pcbi.1004284.

[77]. Oomen PJA, Phung T-KN, Bilchick KC, Holmes JW, Predicting the Outcome of Cardiac Resynchronization Therapy Using a Fast Electromechanical Model, in: Summer Biomech. Bioeng. Biotransport Conf, 2020, pp. 688–689.

[78]. Soepriatna AH, Kevin Yeh A, Clifford AD, Bezci SE, O'Connell GD, Goergen CJ, Three-dimensional myocardial strain correlates with murine left ventricular remodelling severity post-infarction, J. R. Soc. Interface 16 (2019), 10.1098/rsif.2019.0570.

[79]. Damen FW, Berman AG, Soepriatna AH, Ellis JM, Buttars SD, Aasa KL, Goergen CJ, High-frequency 4-dimensional ultrasound (4DUS): a reliable method for assessing murine cardiac function, Tomogr. (Ann Arbor, Mich.) 3 (2017) 180–187, 10.18383/j.tom.2017.00016.

[80]. Sriramula S, Cardinale JP, Lazartigues E, Francis J, ACE2 overexpression in the paraventricular nucleus attenuates angiotensin II-induced hypertension, Cardiovasc. Res 92 (2011) 401–408, 10.1093/cvr/cvr242. [PubMed: 21952934]

[81]. Irvine RJ, White J, Chan R, The Influence on Blood Pressure in the Rat, J. Pharmacol. Toxicol 38 (1998) 157–162.

[82]. Griffin KA, Abu-Amarah I, Picken M, Bidani AK, Renoprotection by ACE inhibition or aldosterone blockade is blood pressure-dependent, Hypertension. 41 (2003) 201–206, 10.1161/01.HYP.0000049881.25304.73. [PubMed: 12574082]

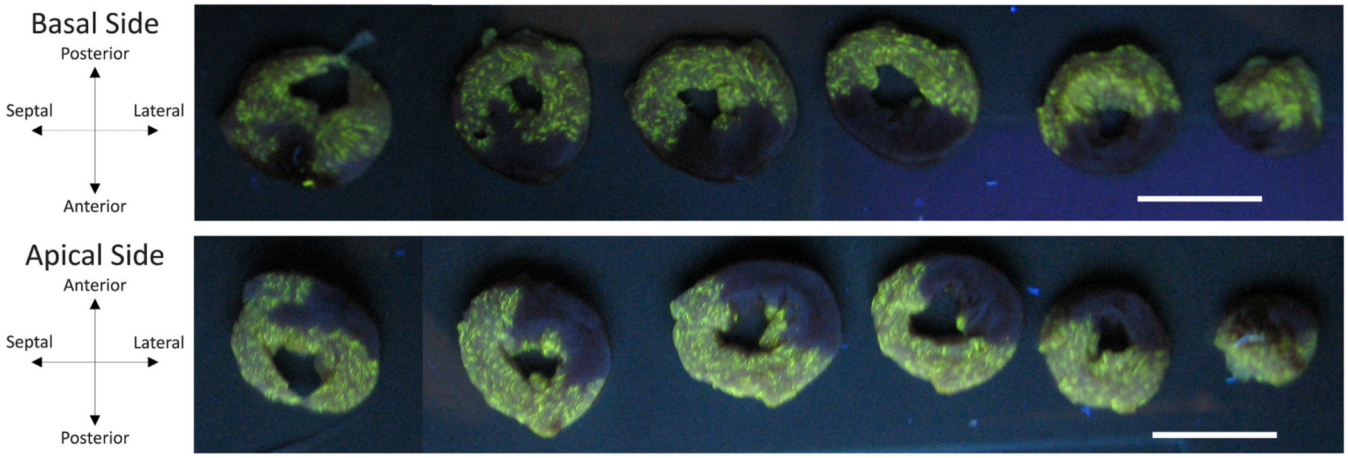

Fig. 1.

Short-axis sections of a representative left ventricle under ultraviolet light following arrest by retrograde perfusion with cold 2,3-butanedione monoxime phosphate-buffered saline containing fluorescent microsphere enables visualization of infarct region. Coronary artery ligation prevented microspheres from reaching infarcted myocardium (dark regions). Scale bars are both 10 mm in length.

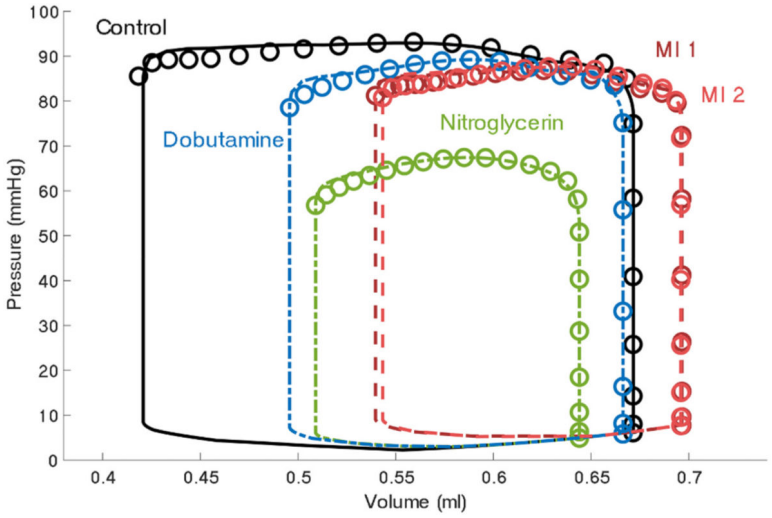

Fig. 2.

Total left ventricle pressure-volume behavior of a representative rat prior to infarction (Time Point 1: Control), following infarction (Time Point 2: MI 1), after nitroglycerin administration (Time Point 3), after drug clearance (Time Point 4: MI 2), and after dobutamine administration (Time Point 5). Data is shown by circles and model fits are shown by solid (Control), dashed (MI 1 or MI 2), or dot-dashed (pharmacologic perturbations) lines.

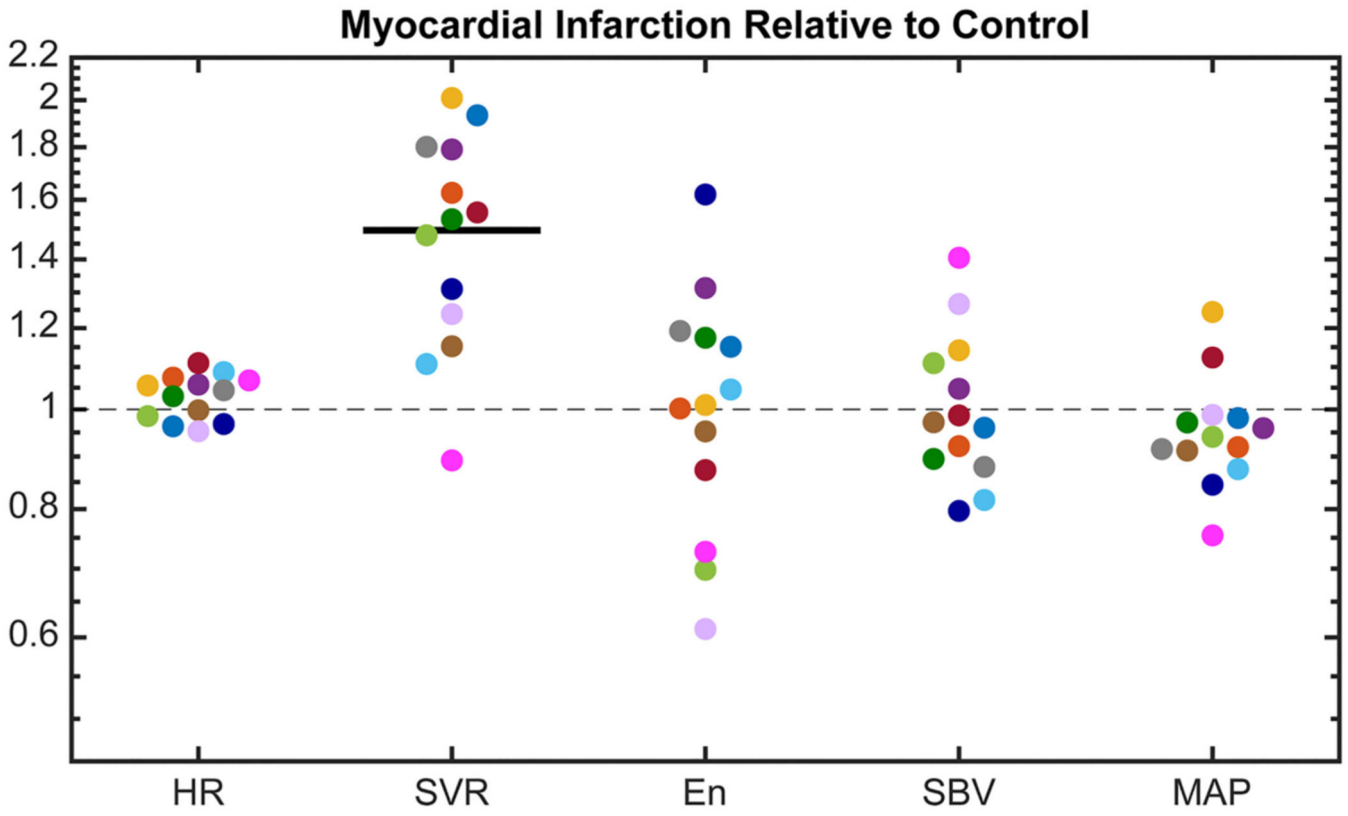

Fig. 3.

Compensatory mechanisms following myocardial infarction, including: measured heart rate (HR), computed systemic vascular resistance (SVR), fitted end-systolic elastance of non-infarcted region (E_n), and fitted stressed blood volume (SBV). Each rat's response is shown in a different color ($n = 13$). The change in computed mean arterial pressure (MAP) is also shown. No change is indicated by the gray dashed line and a significant mean change for all animals is indicated by a dark solid line ($p < 0.05$). Paired parametric t-tests were performed on all metrics except MAP, which failed the normality test and was analyzed with a Wilcoxon matched-pairs signed rank test.

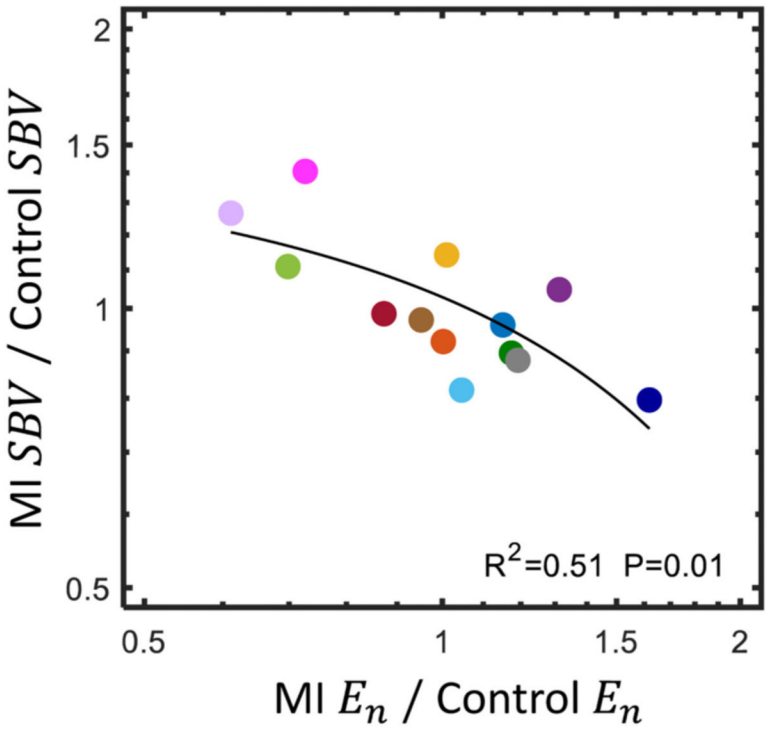

Fig. 4.

There was a significant negative relationship between the change in SBV and the change in E_n from control following myocardial infarction, MI, (two-tailed Pearson correlation coefficient, passed test for homoscedasticity). The linear regression line appears curved because of the logarithmic axes.

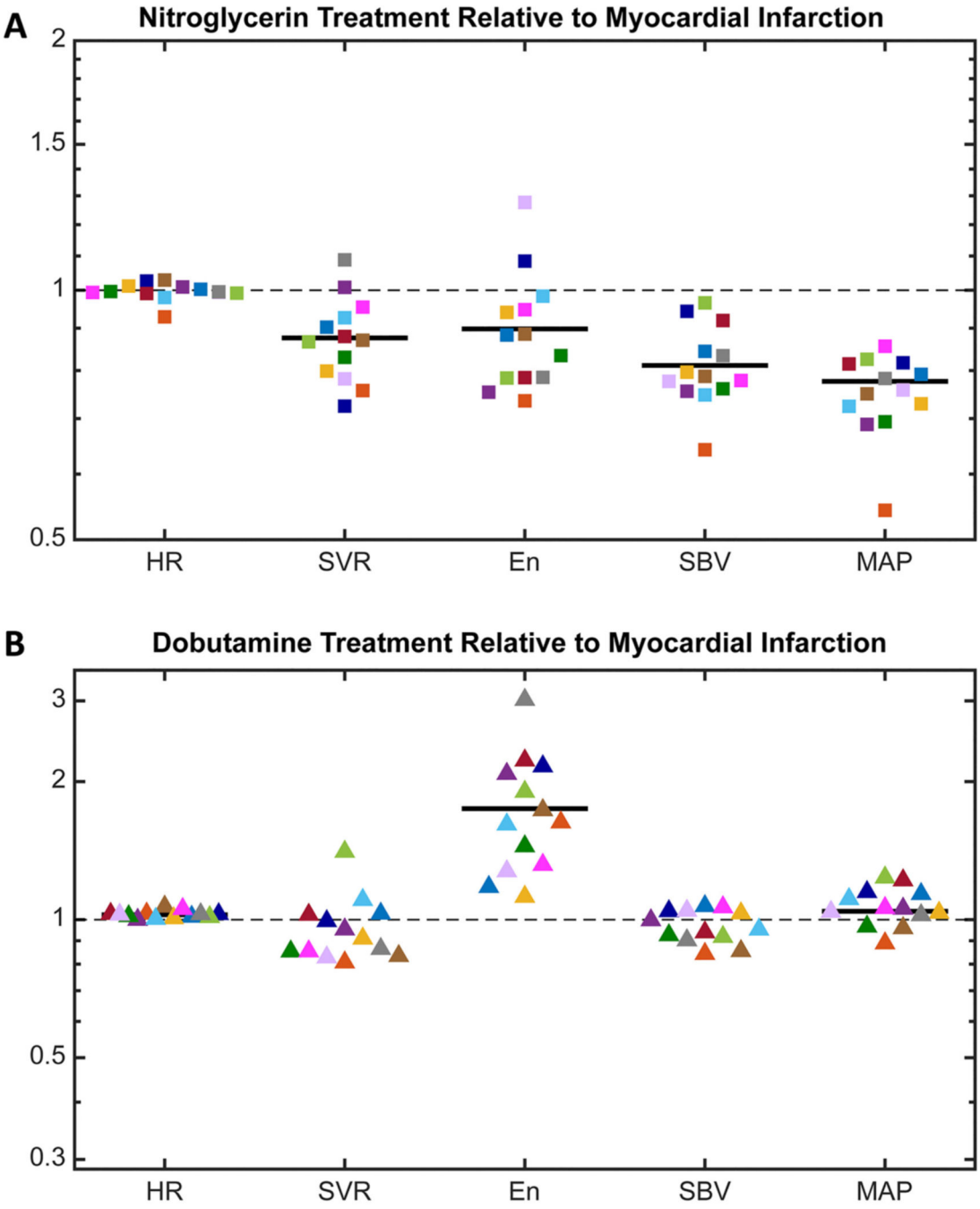

Fig. 5.

(A) Change in the postinfarction compensatory response with the administration of nitroglycerin, including: measured heart rate (HR), computed systemic vascular resistance (SVR), fitted end-systolic elastance of the non-infarcted region E_n, and fitted stressed blood volume (SBV). The change in computed mean arterial pressure (MAP) from postinfarction is also shown. (B) Change in the postinfarction compensatory response with the administration of dobutamine. For both nitroglycerin and dobutamine, no change is indicated by the gray dashed line and a significant mean change for all animals is indicated

by a dark solid line ($p < 0.05$). Paired parametric *t*-tests were performed on all metrics except MAP, which failed the normality test and was analyzed with a Wilcoxon matched-pairs signed rank test.

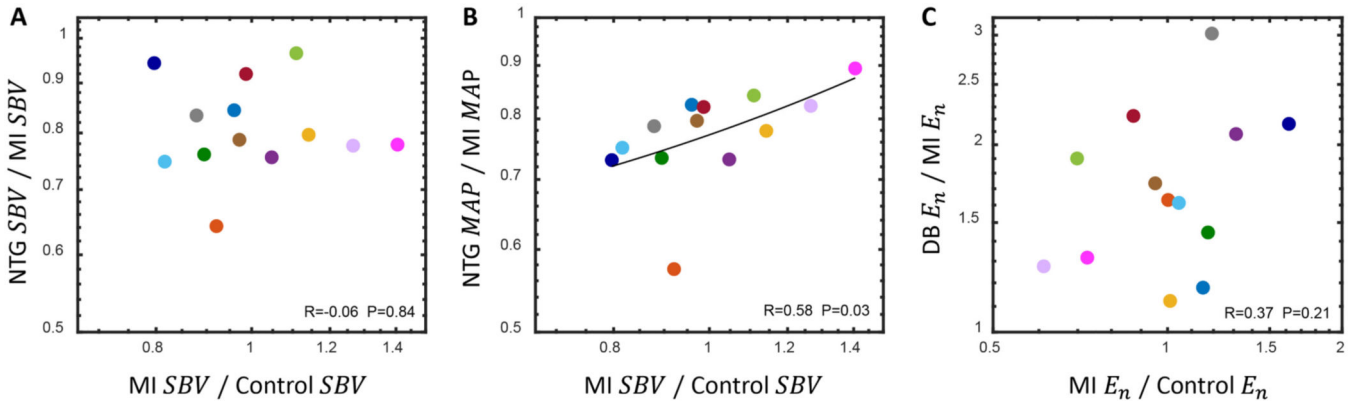

Fig. 6.

(A) The postinfarction reduction in SBV with nitroglycerin (NTG) administration was not correlated with its initial compensatory response (two-tailed Pearson correlation coefficient). (B) The postinfarction reduction in MAP with nitroglycerin administration was correlated with the initial compensatory response of SBV (nonparametric Spearman correlation coefficient). (C) The postinfarction increase in E_n with dobutamine (DB) administration was not correlated with its initial compensatory response (two-tailed Pearson correlation coefficient). Linear regression lines appear curved because of the logarithmic axes. In all cases, linear regression passed the test for homoscedasticity and correlation coefficients were considered significant if $p < 0.05$.

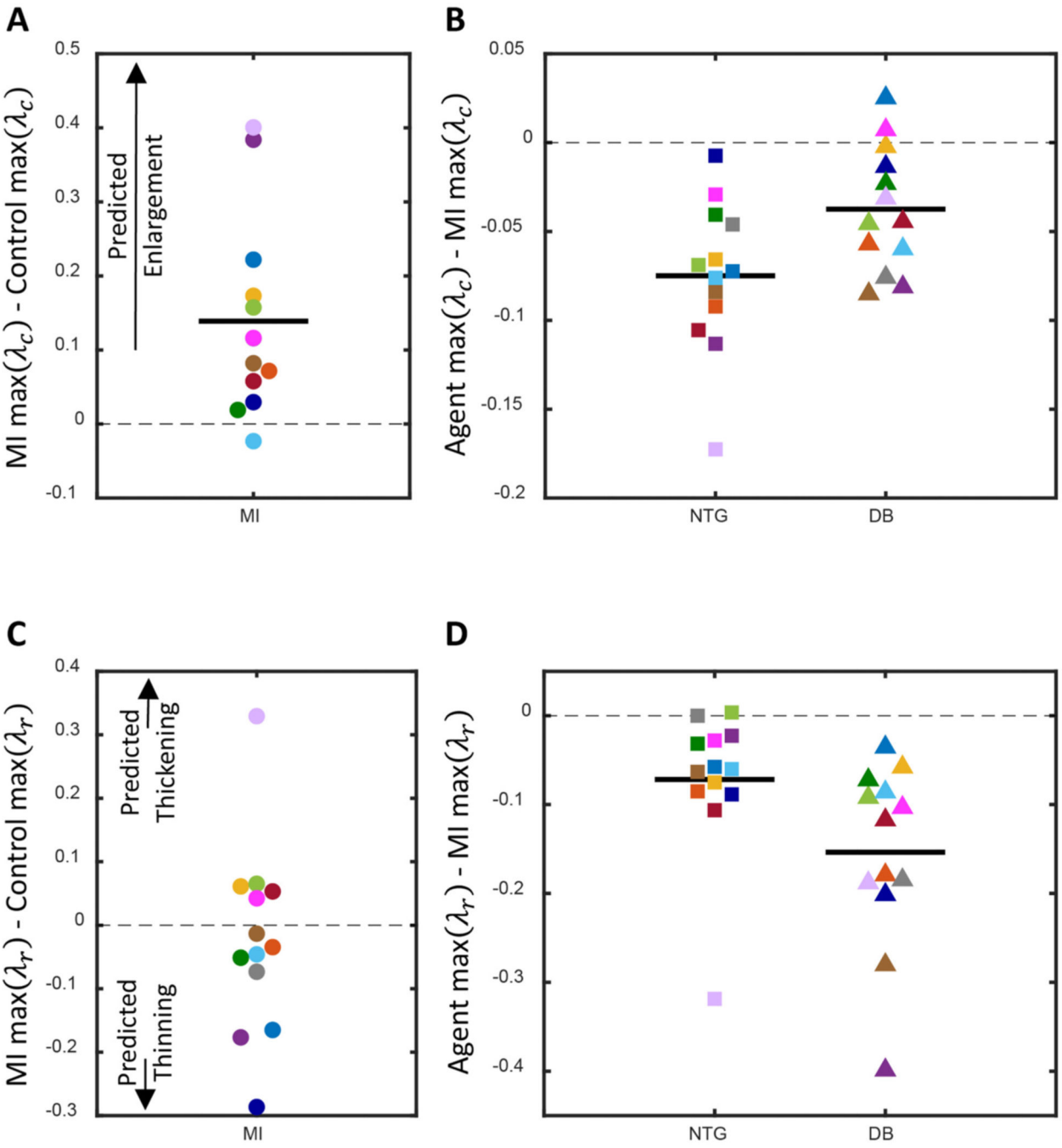

Fig. 7.

(A) The difference in peak circumferential stretch, λ_c, following myocardial infarction (MI). Increased peak λ_c was associated with more ventricular enlargement in prior studies [21,25]. (B) The difference in postinfarction peak λ_c with administration of a pharmacologic agent, either nitroglycerin (NG) or dobutamine (DB). (C) Difference in peak radial stretch, λ_r, following MI. Increased peak λ_r was indicative of ventricular thickening and decreased peak λ_r was indicative of ventricular thinning in prior studies. (D) The difference in postinfarction peak λ_r with administration of NG or DB. In all plots no change is indicated by the gray

dashed line and a significant average difference is indicated by a dark solid line ($p < 0.05$). Paired parametric *t*-tests were performed for all analyses since peak stretches were both normally distributed at all time points. Each rat's response is shown in a different color.

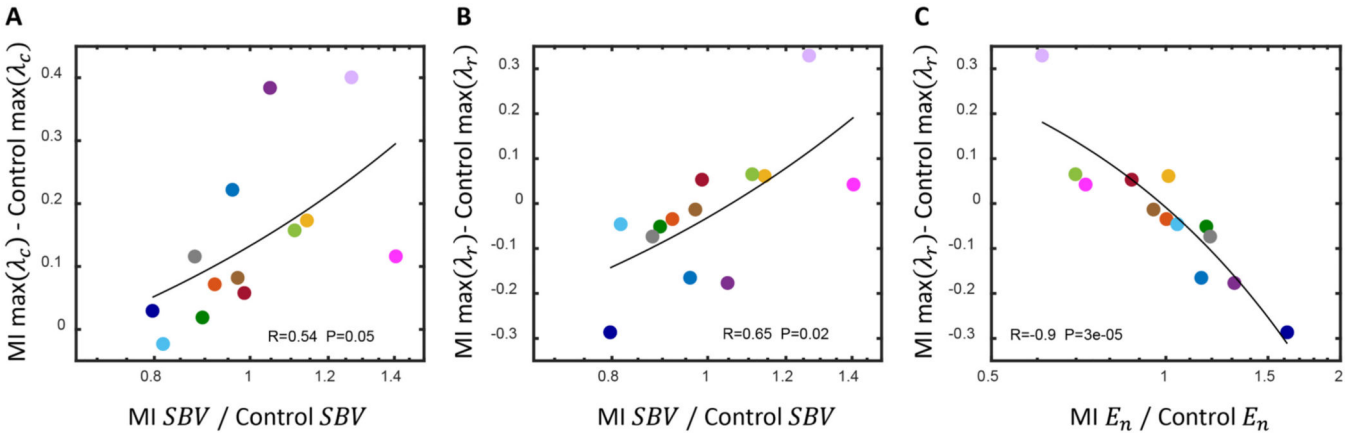

Fig. 8.

(A) There was a significant positive relationship between the postinfarction change in stressed blood volume, SBV, and the difference in peak circumferential stretch, λ_c. (B) There was a significant positive relationship between the postinfarction change in SBV and the difference in peak radial stretch, λ_r. (C) There was a significant negative relationship between the postinfarction change in E_n and the postinfarction difference in peak λ_r. In all cases, linear regression passed the test for homoscedasticity and the two-tailed Pearson correlation coefficients were considered significant if $p < 0.05$.

Table 1

Left ventricular pressure and segment lengths were recorded at five time points in each rat.

Time point	State	Measurement time
1	Control	Prior to Ligation
2	Myocardial Infarction	30 min Following Ligation
3	Myocardial Infarction + Dobutamine (or Nitroglycerin)	Immediately Following Drug Administration
4	Myocardial Infarction 2	5 min Following Drug Administration
5	Myocardial Infarction + Nitroglycerin (or Dobutamine)	Immediately Following Drug Administration